

Electronic supporting Information

**Highly efficient cobalt catalysts promoted by CeO₂-Al₂O₃ for ammonia
decomposition**

Kai Xu,^{† a, b} Na Jiang,^{† b} Peng Wang,^a Wei-Wei Wang,^{* b} Chun-jiang Jia^{* b}

^aState Key Laboratory of Crystal Materials, Shandong University, Jinan 250100, China.

^bKey Laboratory for Colloid and Interface Chemistry, Key Laboratory of Special Aggregated Materials, School of Chemistry and Chemical Engineering, Shandong University, Jinan 250100, China.

† These authors contributed equally: Kai Xu, Na Jiang.

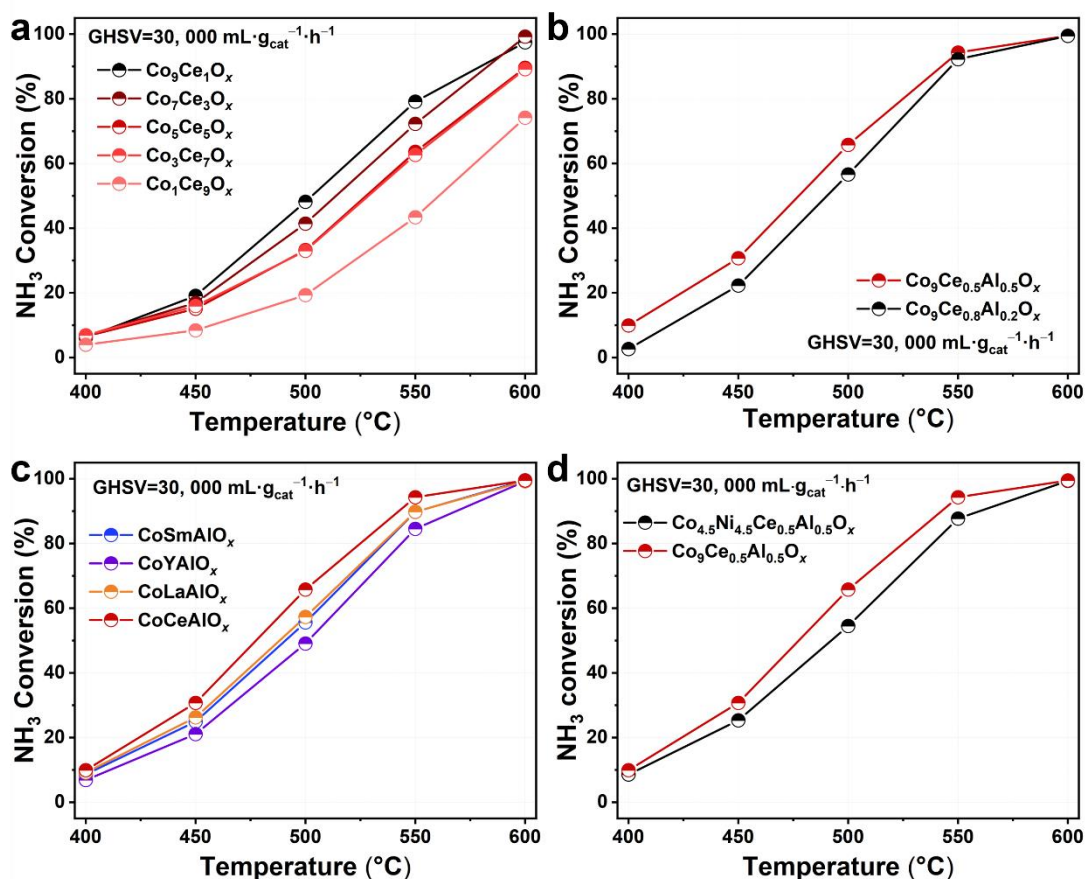


Fig. S1 Temperature-dependent activities of the Co-based catalysts. (a) CoCeO_x catalysts with different Co/Ce ratio; (b) CoCeAlO_x catalysts with different Ce/Al ratio; (c) Co₉RE_{0.5}Al_{0.5}O_x catalysts with different rare earth elements (Sm, Y, La, Ce); (d) Co_{4.5}Ni_{4.5}Ce_{0.5}Al_{0.5}O_x and Co₉Ce_{0.5}Al_{0.5}O_x

To investigate the impact of component concentrations on the ammonia decomposition reaction, we assessed the reactivity of the catalysts with different mole ratios of Co, Ce and Al element. As the ratio of Co:Ce decreased (Fig. S1a), a pronounced decline in activity of the Co_aCe_bO_x catalysts occurred. Therefore, it is inferred that cobalt species was the main active species for ammonia decomposition, whilst ceria acted as an assisting promoter. From Fig. S1b, it could be observed that the second round NH₃ conversion of Co₉Ce_{0.8}Al_{0.2}O_x decreased by approximately 9% as the mole ratio reduced from 0.5 to 0.2. This indicated the vital role of alumina in preserving stability of activity. Additionally, the catalysts obtained by replacing Ce with other rare earth elements delivered inferior activity compared to CoCeAlO_x, demonstrating the unique advantages of Ce for applying in ammonia decomposition reaction (Fig. S1c). And Co_{4.5}Ni_{4.5}Ce_{0.5}Al_{0.5}O_x showed lower activity than Co₉Ce_{0.5}Al_{0.5}O_x (Fig. S1d).

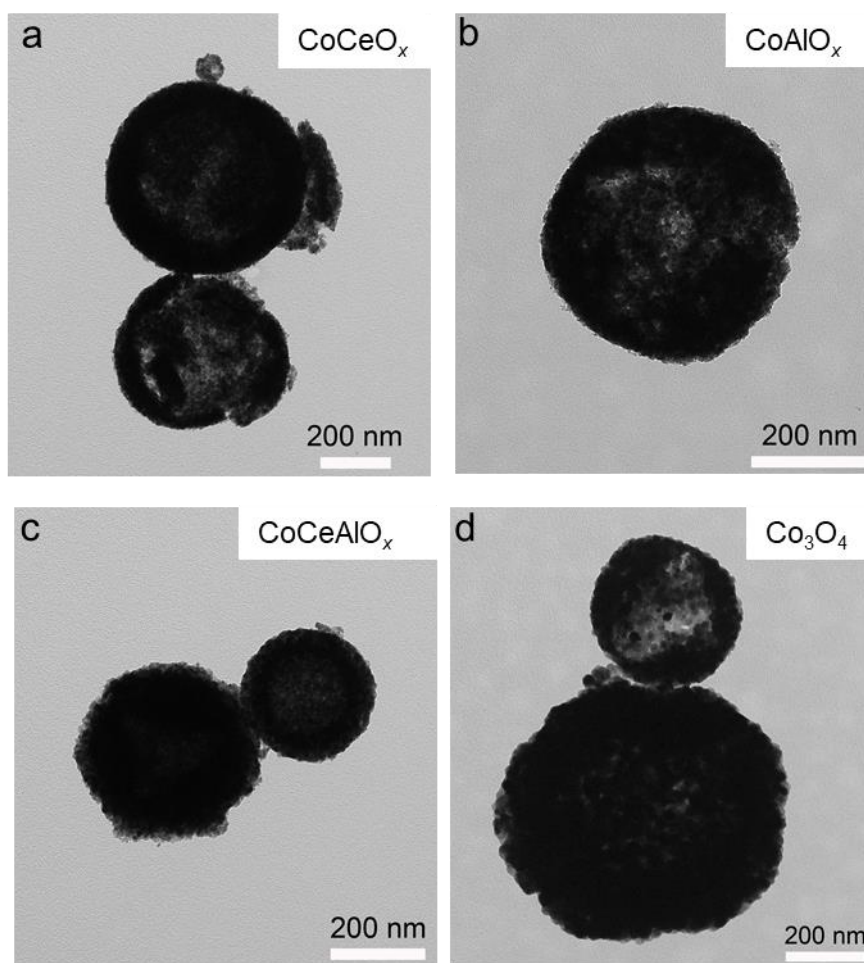


Fig. S2 TEM images of the as-prepared samples. (a) CoCeO_x ; (b) CoAlO_x ; (c) CoCeAlO_x ; (d) Co_3O_4

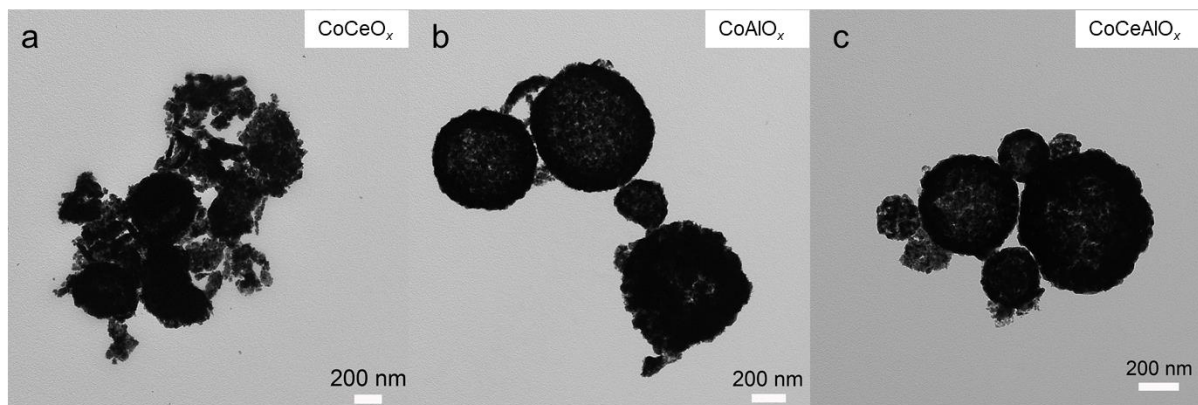


Fig. S3 TEM images of the used samples. (a) CoCeO_x; (b) CoAlO_x; (c) CoCeAlO_x

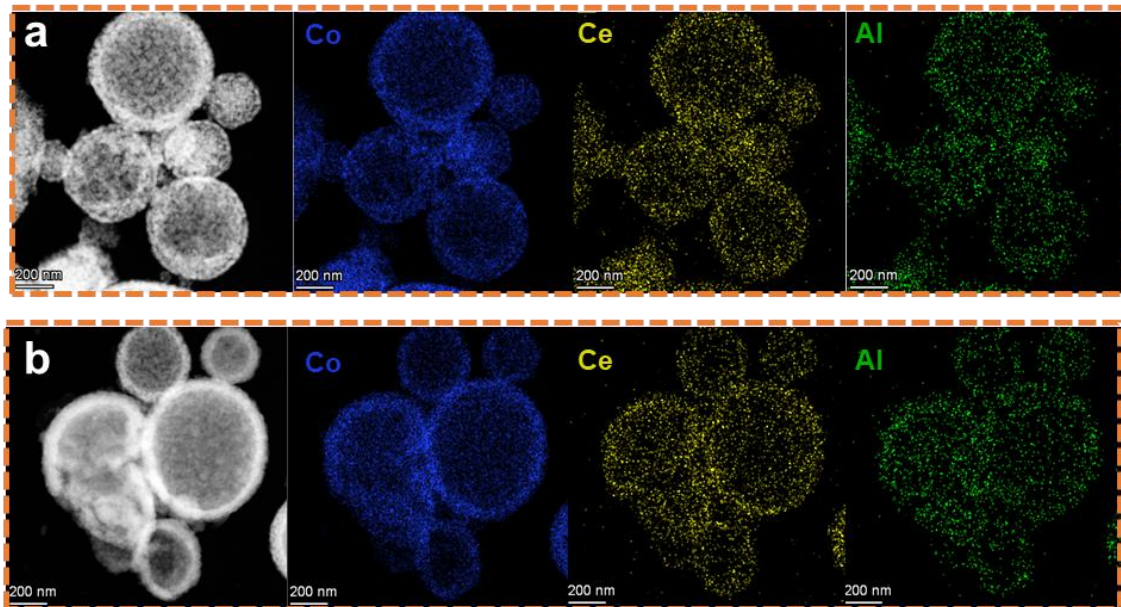


Fig. S4 The EDS elemental mappings of the CoCeAlO_x sample after long-term stability tests

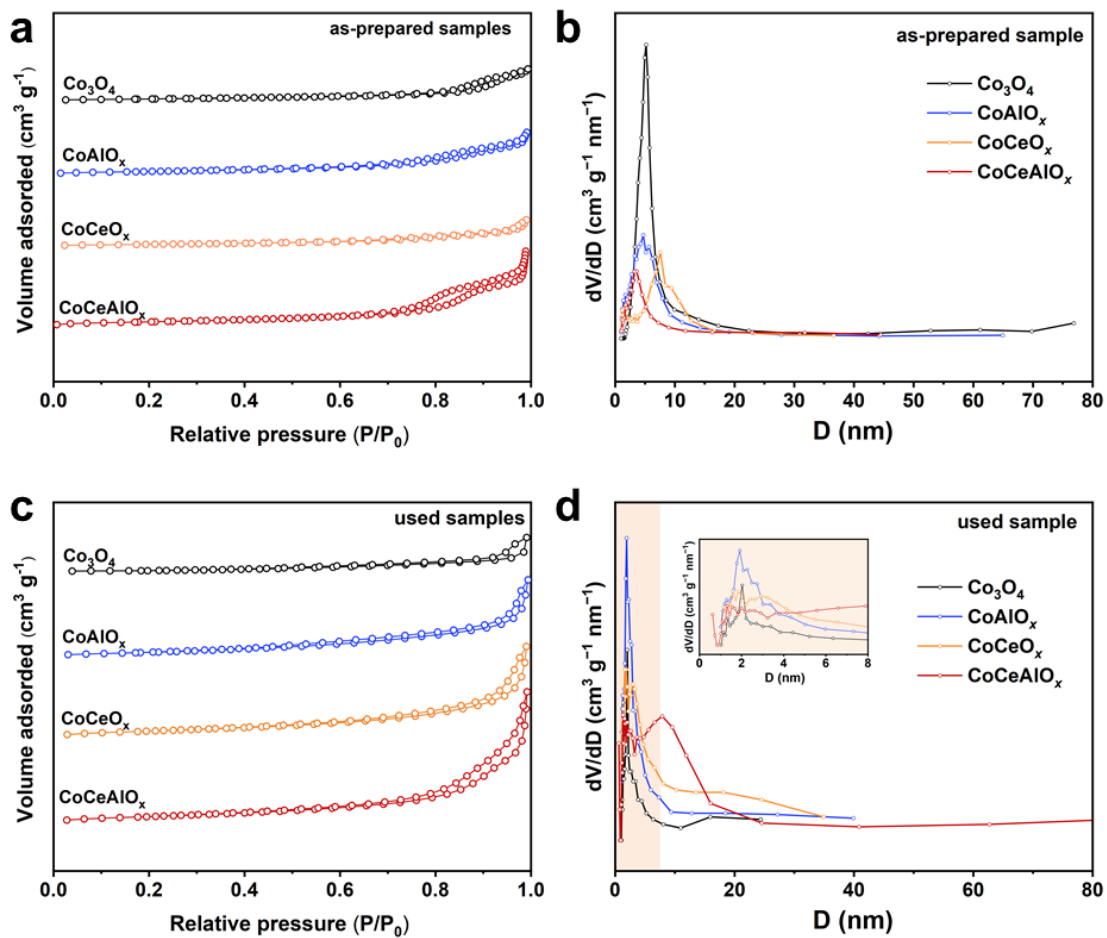


Fig. S5 The physical properties of the catalysts. (a, c) The N₂ adsorption-desorption isotherms of the as-prepared (a) and used (c) samples; (b, d) BJH pore size distributions of the as-prepared (b) and used (d) samples

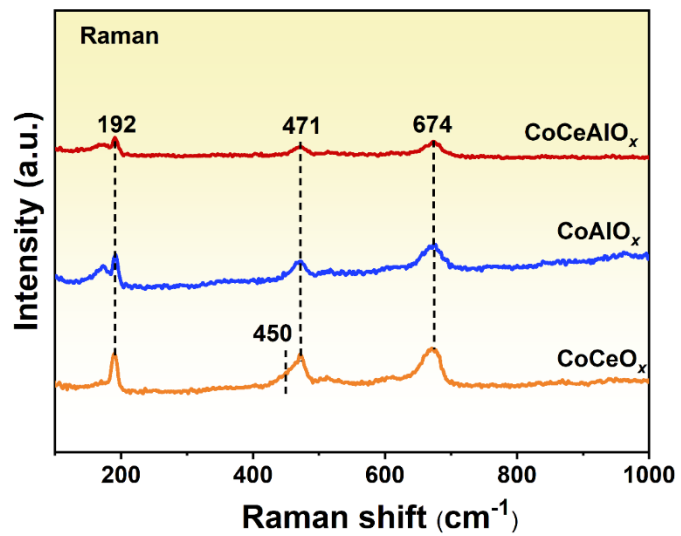


Fig.S6 The Raman spectra of the samples after long-term stability tests

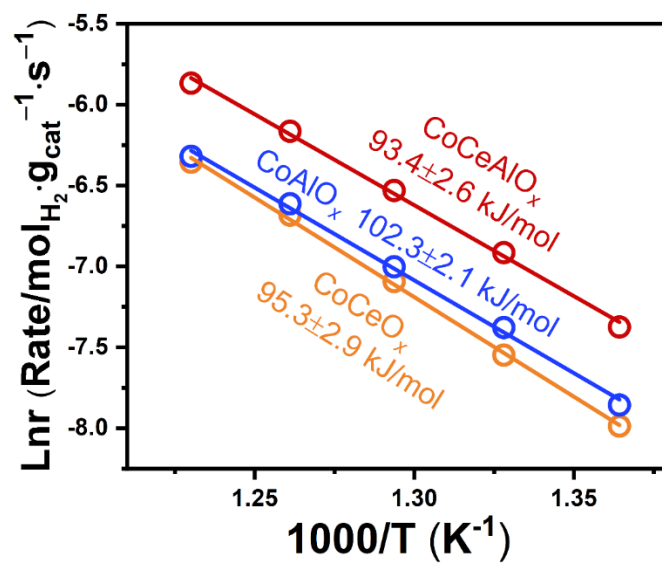


Fig.S7 Arrhenius plots for the catalysts (CoCeAlO_x, CoCeO_x and CoAlO_x) in the kinetic range

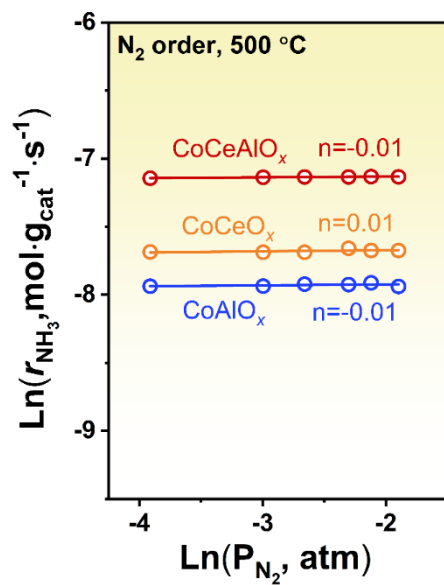


Fig. S8 The Reaction orders of the N₂ for CoCeAlO_x, CoCeO_x and CoAlO_x

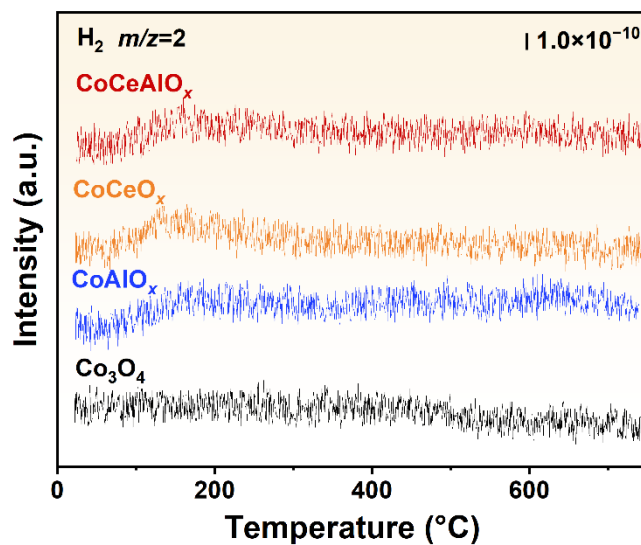


Fig. S9 The desorption signals of H₂ ($m/z=2$) in NH₃-TPD over CoCeAlO_x, CoCeO_x, CoAlO_x and Co₃O₄ catalysts.

The H₂ signal of all related samples was shown in Fig. S9. It exhibited poor data quality, causing no efficient information could be obtained. The greater capacity of CoCeAlO_x for the suppression of hydrogen poisoning could be clearly concluded by the reaction order of H₂ (Fig. 7b).

Table S1 The ICP-AES results of various samples.

| Samples | Co loading (wt%) | Ce loading (wt%) | Al loading (wt%) |
|----------------------|------------------|------------------|------------------|
| CoCeAlO _x | 60.0 | 7.4 | 2.4 |
| CoCeO _x | 58.1 | 13.1 | — |
| CoAlO _x | 66.6 | — | 5.8 |

Table S2 Physical properties of the as-prepared samples.

| Catalysts | Surface area (m ² g ⁻¹) ^a | Size of Co ₃ O ₄ (nm) ^b | Size of CeO ₂ (nm) ^b |
|--------------------------------|---|--|--|
| CoCeAlO _x | 119.4 | 8.7 | \ |
| CoAlO _x | 83.3 | 15.2 | \ |
| CoCeO _x | 54.0 | 9.6 | 5.4 |
| Co ₃ O ₄ | 46.6 | 17.1 | \ |

a Measured by N₂ adsorption-desorption experiments.

b Evaluated by XRD results using Debye-Scherrer equation.

Table S3 Physical properties of the used samples.

| Catalysts | Surface area (m ² g ⁻¹) ^a | Size of Co (nm) ^b | Size of CeO ₂ (nm) ^b |
|--------------------------------|---|------------------------------|--|
| CoCeAlO _x | 40.1 | 10.3 | \ |
| CoAlO _x | 30.0 | 15.3 | \ |
| CoCeO _x | 38.2 | 21.2 | 9.1 |
| Co ₃ O ₄ | 5.7 | 32.0 | \ |

a Measured by N₂ adsorption-desorption experiments.

b Evaluated by XRD results using Debye-Scherrer equation.

Table S4 The peak center of different Co species (Co^{3+} , Co^{2+} , Co^0) in XPS.

| Samples | Binding Energy (eV) | | |
|--------------------|---------------------|------------------|---------------|
| | Co^{3+} | Co^{2+} | Co^0 |
| CoCeAlO_x | 779.8, 794.8 | 781.5, 796.5 | 778.3, 793.3 |
| CoCeO_x | 779.8, 794.8 | 781.5, 796.5 | 778.4, 793.4 |
| CoAlO_x | 780.1, 795.1 | 781.8, 796.8 | 778.3, 793.3 |

Table S5 The peak center of different Ce species (Ce^{3+} , Ce^{4+}) in XPS.

| Samples | Binding Energy (eV) | |
|--------------------|----------------------------|--|
| | Ce^{3+} | Ce^{4+} |
| CoCeAlO_x | 903.9, 899.0, 885.4, 880.5 | 916.3, 907.3, 900.7, 897.8, 888.8, 882.2 |
| CoCeO_x | 903.9, 899.3, 885.4, 880.8 | 916.3, 907.6, 900.7, 897.8, 889.1, 882.2 |

Table S6 The elements and surface composition analyzed by the XPS data of the used catalysts

| Catalysts | $\text{Co}^0 / (\text{Co}^{3+} + \text{Co}^{2+} + \text{Co}^0)$ | $\text{Ce}^{3+} / (\text{Ce}^{3+} + \text{Ce}^{4+})$ |
|--------------------|---|--|
| CoCeAlO_x | 19.1% | 34.5% |
| CoAlO_x | 22.1% | \ |
| CoCeO_x | 16.0% | 27.5% |